

## Supporting Information

# The influence of H<sub>2</sub>O or/and O<sub>2</sub> introduction during the low-temperature gas-phase sulfation of organic COS+CS<sub>2</sub> on the conversion and deposition of sulfur-containing species in the sulfated CeO<sub>2</sub>-OS catalyst for NH<sub>3</sub>-SCR

Zhibo Xiong<sup>1\*</sup>, Yafei Zhu<sup>1</sup>, Jiaxing Liu<sup>1</sup>, Yanping Du<sup>2</sup>, Fei Zhou<sup>3</sup>, Jing Jin<sup>1\*\*</sup>, Qiguo Yang<sup>1\*\*</sup>, Wei Lu<sup>1</sup>

1. School of Energy and Power Engineering, University of Shanghai for Science & Technology, Shanghai, 200093, China

2. School of Engineering, Lancaster University, Lancaster, LA1 4YW, UK

3. Jiangsu Guoxin Jingjiang Power Co. Ltd., Jingjiang 214500, Jiangsu, China

## Catalyst characterization

The BET specific surface area, pore diameter and pore volume of catalysts were determined by N<sub>2</sub> adsorption-desorption analysis at 77 K using a micromeritics ASAP 2460 system instrument. The crystal phase diffraction pattern of catalysts was identified on the 6100 X-ray diffraction Analyzer with Cu K $\alpha$  radiation (model D/max RA, Rigaku Co., Japan). The scanning range (2 $\theta$ ) was collected from 10 ° to 80 ° at a scanning velocity of 5 °/min. The Raman spectra of samples were collected at a Raman Spectrometer (InVia Reflex, Renishaw), using a laser at 532 nm line as the excitation source. The surface morphology and structure of catalysts were observed by scanning electron microscopy (SEM) on a ZEISS SIGMA HD instrument. Transmission electron microscopy (TEM) was performed on a Thermo Fischer Talos F200x instrument with an operating voltage of 200 kV.

X-ray photoelectron spectroscopy (XPS) was performed to acquire the surface element information of the samples, which was conducted on ThermoFisher Scientific Escalab 250Xi using an Al K $\alpha$  X-ray source with an excitation energy of 1486.7 eV. The energy calibration of all elements were calibrated by normalizing the C 1s line of adsorbed amorphous hydrocarbons to 284.8 eV, and the spectra was fitted by XPS PEAK software with Gaussian-Lorentz function.

H<sub>2</sub> temperature programmed reduction (H<sub>2</sub>-TPR) and NH<sub>3</sub> temperature programmed desorption (NH<sub>3</sub>-TPD) experiments were carried out on AutoChem II with TCD detection (Micromeritics, USA). For H<sub>2</sub>-TPR, 100 mg samples were pretreated at 300 °C for 30 min in Ar

atmosphere and then cooled to 50 °C. Subsequently, the data were collected at a heating rate of 10 °C/min from 50 to 900 °C in a 10% H<sub>2</sub>-Ar (40 mL/min) atmosphere. In NH<sub>3</sub>-TPD, 100 mg samples were pretreated at 500 °C for 1 h in He atmosphere and then cooled to 35 °C. The sample was purged with 10% NH<sub>3</sub>/He (50 mL/min) for 2 h at 35 °C, and then purged with high purity He for 1 h to remove the physical adsorption species. Finally, the desorption processes were initiated from 35 to 500 °C with a ramp rate of 10 °C/min.

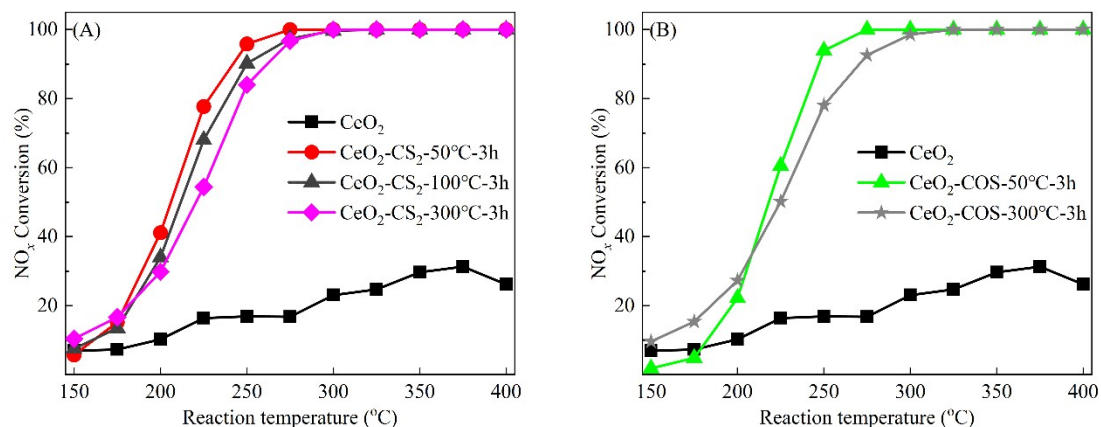


**Fig. S1.** Influence of sulfation temperature on the  $\text{NH}_3$ -SCR activity of the gas-phase sulfated  $\text{CeO}_2$  catalysts by organic sulfur ((A)  $\text{CS}_2$ , (B)  $\text{COS}$ ).

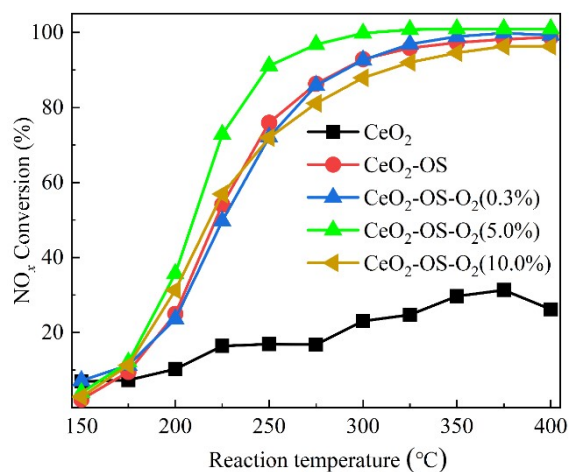


**Fig. S2.** Influence of oxygen concentration on the  $\text{NH}_3$ -SCR activity of the sulfated  $\text{CeO}_2\text{-OS}$  catalyst by the organic  $\text{CS}_2\text{+COS}$  at  $50^{\circ}\text{C}$ . The simulated flue gas components during the sulfation:  $\text{CS}_2$  30 ppm +  $\text{COS}$  140 ppm (when used,  $\text{COS}:\text{CS}_2=7:3$ );  $\text{O}_2=0.3$  vol.%, 5.0 vol.%, 10.0 vol.% (when used); pretreated at  $50^{\circ}\text{C}$  for 3 h.

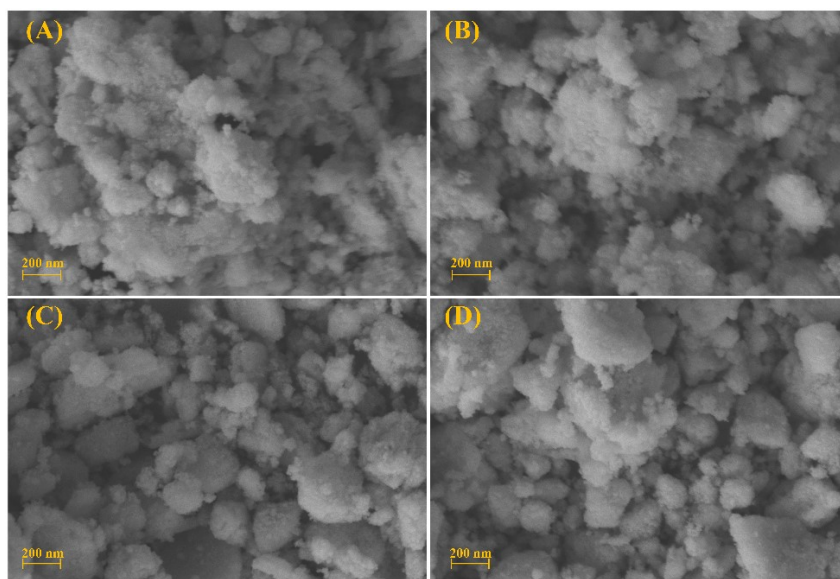


**Fig. S3.** The SEM images of (A)  $\text{CeO}_2\text{-OS}$ , (B)  $\text{CeO}_2\text{-OS-O}_2$ , (C)  $\text{CeO}_2\text{-OS-H}_2\text{O}$  and (D)  $\text{CeO}_2\text{-OS-O}_2\text{+H}_2\text{O}$  catalysts.

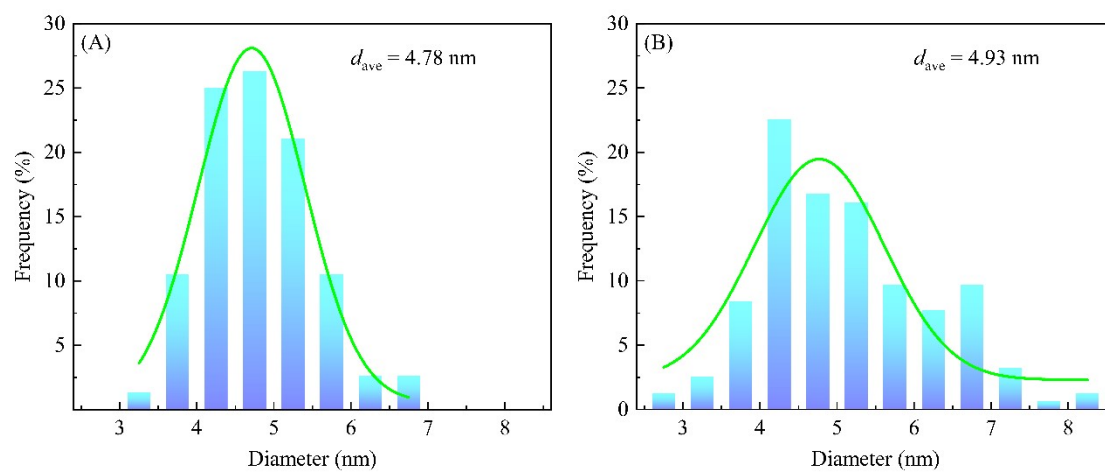


**Fig. S4.** Particle size distributions of  $\text{CeO}_2$  and  $\text{CeO}_2\text{-OS-O}_2\text{+H}_2\text{O}$  catalysts.

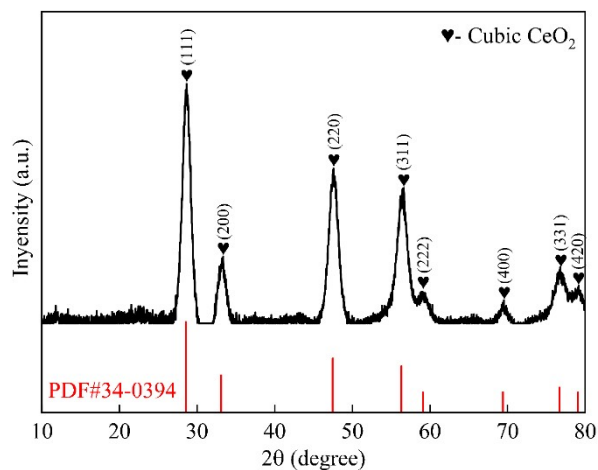


**Fig. S5.** The XRD patterns of the as-prepared CeO<sub>2</sub> catalyst.

**Table S1.** The chosen O<sub>2</sub> concentrations for the hydrolysis of organic COS/CS<sub>2</sub>

Catalysts	O <sub>2</sub> concentrations	Optimal O <sub>2</sub> concentrations	GHSV	Ref.
Cu-Fe/TSAC	0%, 0.5%, 1%, 5%	0.5%	10000 /h	[1]
Cu-K-Co/AC	0%, 0.1%, 0.2%	0.1%	30000 /h	[2]
Al <sub>2</sub> O <sub>3</sub> -K/CAC	0%, 1.5%, 5.5%	1.5%	10000 /h	[3]
La <sub>2</sub> O <sub>3</sub> S, Nd <sub>2</sub> O <sub>3</sub> S	0%, 0.25%, 0.5%, 1%, 1.5%, 2%	0.5%, 1%, 1.5%	10000 /h	[4]
NaOH/Al <sub>2</sub> O <sub>3</sub>	0%, 1%, 2%, 3%	0%	220000 /h	[5]

**Table S2.** Hydrolysis conditions and properties of different catalysts for organic COS/CS<sub>2</sub>

Catalysts	Test condition	t <sub>90</sub> (min)	Ref.
MgAlCeO <sub>x</sub>	COS=470 ppm, T=50 °C, GHSV=5000 /h	100	[6]
ZnAl-20Sm-Na MMO	COS=400 ppm, T=60 °C, WHSV=7500 mL/(g·h)	160	[7]
Ni-mAl <sub>2</sub> O <sub>3</sub>	COS=300 ppm, T=70 °C, GHSV=9000 /h	150	[8]
5%Fe/MCAC	COS=400 ppm, T=70 °C, GHSV=6000 /h	210	[9]
10-KA	COS=400 ppm, T=50 °C, GHSV=20000 /h	300	[10]
K <sub>0.1</sub> Al <sub>2</sub> O <sub>3</sub> -PA	COS=200 ppm, T=50~150 °C, GHSV=24000 /h	-	[11]
K@Al	COS=150 ppm, CS <sub>2</sub> =50 ppm, T=80~160 °C, GHSV=20000/h	-	[12]
Ni(5)ACF(400)	COS=400 ppm, CS <sub>2</sub> =50 ppm, T=60 °C, GHSV=10000 /h	-	[13]
CSB-XXY	COS=450 ppm, CS <sub>2</sub> =40 ppm, T=150 °C, GHSV=10000 /h	-	[14]

## References

- [1] X. Sun, H. T. Ruan, X. Song, L. N. Sun, K. Li, P. Ning, C. Wang, Research into the reaction process and the effect of reaction conditions on the simultaneous removal of H<sub>2</sub>S, COS and CS<sub>2</sub> at low temperature, *RSC Adv.*, 2018, 8, 6996.
- [2] X. Li, X. Q. Wang, L. L. Wang, P. Ning, Y. X. Ma, L. Zhong, Y. Wu, L. Yuan, Efficient removal of carbonyl sulfur and hydrogen sulfide from blast furnace gas by one-step catalytic process with modified activated carbon, *Appl. Surf. Sci.*, 2022, 579, 152189.
- [3] X. Sun, P. Ning, X. L. Tang, H. H. Yi, K. Li, D. He, X. M. Xu, B. Huang, R. Y. Lai, Simultaneous catalytic hydrolysis of carbonyl sulfide and carbon disulfide over Al<sub>2</sub>O<sub>3</sub>-K/CAC catalyst at low temperature, *J. Energy Chem.*, 2014, 23, 221-226.
- [4] Y. Q. Zhang, Z. B. Xiao, J. X. Ma, Hydrolysis of carbonyl sulfide over rare earth oxysulfides, *Appl. Catal., B*, 2004, 48, 57-63.
- [5] Q. Cao, Y. T. Lin, Y. R. Li, J. L. Tian, H. Q. Liu, T. Y. Zhu, J. C. Wang, Hydrolysis of Carbonyl Sulfide in Blast Furnace Gas Using Alkali Metal-Modified  $\gamma$ -Al<sub>2</sub>O<sub>3</sub> Catalysts with High Sulfur Resistance, *ACS Omega*, 2023, 8, 35608-35618.
- [6] X. Song, L. N. Sun, H. B. Guo, K. Li, X. Sun, C. Wang, P. Ning, Experimental and Theoretical Studies on the influence of Carrier Gas for COS Catalytic Hydrolysis over MgAlCe Composite Oxides, *ACS Omega*, 2019, 4, 7122-7127.
- [7] S. J. Hu, J. N. Gu, K. Li, J. X. Liang, Y. X. Xue, X. Min, M. M. Guo, X. F. Hu, J. P. Jia, T. H. Sun, Boosting COS catalytic hydrolysis performance over Zn-Al oxide derived from ZnAl hydrotalcite-like compound modified via the dopant of rare earth metals and the replacement of precipitation base, *Appl. Surf. Sci.*, 2022, 599, 154016.
- [8] H. K. Jin, Z. Y. An, Q. C. Li, Y. Q. Duan, Z. H. Zhou, Z. K. Sun, L. B. Duan, Catalysts of Ordered Mesoporous Alumina with a Large Pore Size for Low-Temperature Hydrolysis of Carbonyl Sulfide, *Energy Fuels*, 2021, 35, 8895-8908.
- [9] P. Ning, K. Li, H. H. Yi, X. L. Tang, J. H. Peng, D. He, H. Y. Wang, S. Z. Zhao, Simultaneous Catalytic Hydrolysis of Carbonyl Sulfide and Carbon Disulfide over Modified Microwave Coal-Based Active Carbon Catalysts at Low Temperature, *J. Phys. Chem. C*, 2012, 116, 17055-17062.
- [10] J. N. Gu, J. X. Liang, S. J. Hu, Y. X. Xue, X. Min, M. M. Guo, X. F. Hu, J. P. Jia, T. H. Sun, Enhanced removal of COS from blast furnace gas via catalytic hydrolysis over Al<sub>2</sub>O<sub>3</sub>-based catalysts: Insight into the role of alkali metal hydroxide, *Sep. Purif. Technol.*, 2022, 295, 121356.

- [11] P. Wu, Y. P. Zhang, Y. L. Liu, H. Q. Yang, K. Shen, G. B. Li, S. Wang, S. P. Ding, S. L. Zhang, Experimental and theoretical research on pore-modified and K-doped  $\text{Al}_2\text{O}_3$  catalysts for COS hydrolysis: The role of oxygen vacancies and basicity, *Chem. Eng. J.*, 2022, 450, 138091.
- [12] R. Cao, X. Q. Wang, P. Ning, Y. B. Xie, L. L. Wang, Y. X. Ma, X. Li, H. Zhang, J. Y. Liu, Advantageous Role of N-doping on K@Al in COS/ $\text{CS}_2$  Hydrolysis: Diminished Oxygen Mobility and Rich basic sites, *Fuel*, 2023, 337, 126882.
- [13] K. L. Li, C. Wang, P. Ning, K. Li, X. Sun, X. Song, Y. Mei, Surface characterization of metal oxides-supported activated carbon fiber catalysts for simultaneous catalytic hydrolysis of carbonyl sulfide and carbon disulfide, *J. Environ. Sci.*, 2020, 96, 44-54.
- [14] N. Liu, X. Song, C. Wang, K. Li, P. Ning, X. Sun, F. Wang, Y. X. Ma, Surface characterization study of corn-straw biochar catalysts for the simultaneous removal of HCN, COS, and  $\text{CS}_2$ , *New J. Chem.*, 2020, 44, 13565.